

A Facile Synthesis of $\text{TiO}_2\text{-NiCo}_2\text{S}_4\text{-Ti}_3\text{C}_2$ Electrode material by Hydrothermal Method and its electrochemical performance for Supercapacitor Application

Chunyong Zhang^{1,2,*}, Yiwen Zhang^{1,2}, Chunzhi Zheng^{1,3,*}, Zhe Li^{1,2}, Haoyu Wang^{1,2}, Haitao Liu^{1,2}, Hengfei Qin^{1,3}

¹ Jiangsu Key Laboratory of Precious Metal Chemistry and Technology, Jiangsu University of Technology, Changzhou, 213001, China

² School of Chemistry and Environmental Engineering, Jiangsu University of Technology, Changzhou, 213001, China

³ Jiangsu Province Key Laboratory of E-Waste Recycling, Jiangsu University of Technology, Changzhou, 213001, China

Yiwen Zhang, Chunyong Zhang contributed equally to this work and should be considered as co-first authors.

* E-mail: zhangcy@just.edu.cn, zhengcz@jsut.edu.cn

Received: 1 May 2022 / Accepted: 7 June 2022 / Published: 7 August 2022

In this paper, using titanium carbide, nickel chloride hexahydrate, cobalt chloride hexahydrate and thiosemicarbazide as raw materials, a kind of electrode material for supercapacitor was prepared by hydrothermal method. The composition and microstructure of the composite material were analyzed by XRD and SEM, and the electrochemical performance of the material was tested by electrochemical workstation. It includes cyclic voltammetry curve, constant current charge-discharge curve and impedance test. The electrochemical test results show that the specific capacitance of the prepared $\text{TiO}_2\text{-NiCo}_2\text{S}_4\text{-Ti}_3\text{C}_2$ electrode can reach 1527.5 F/g at the scanning rate of 5 mV/s, which is higher than that of the contrast Ti_3C_2 , $\text{TiO}_2\text{-Ti}_3\text{C}_2$ and $\text{NiCo}_2\text{S}_4\text{-Ti}_3\text{C}_2$ electrode materials.

Keywords: Ti_3C_2 ; Composite materials; Supercapacitor; Electrochemical performance

1. INTRODUCTION

With the development of economy and social progress, human's demand for energy is increasing day by day, resulting in a large amount of energy consumption and serious pollution to the environment. Non-renewable resources such as coal and oil are increasingly in short supply. In addition, the burning of fossil fuels will cause many problems such as environmental pollution, greenhouse effect and global warming and reduce people's quality of life and health. In order to alleviate the crisis of traditional energy

exhaustion and improve human living environment, human beings begin to seek new clean and renewable energy. Solar energy, wind energy, tidal energy and other renewable clean energy have been widely applied, which can greatly slow down the consumption of non-renewable energy, but also can achieve low pollution and create a comfortable living environment. However, due to the influence of regional and climatic factors, energy storage and transportation are intermittent and cannot provide a sustainable energy supply, which greatly limits its application. Therefore, people began to study energy storage devices. Among all kinds of electrochemical energy storage, supercapacitors have attracted wide attention due to their advantages of fast charging and discharging rate, long cycle life, environmental protection, high power density and high efficiency [1-4]. Electrode materials for supercapacitors can be divided into three categories: carbon material series, transition metal oxide series and conductive polymer series [5]. Graphene, as one of the carbon materials, has been deeply studied in the field of electrode materials due to its advantages of high conductivity, good electrochemical stability and high specific surface area, and shows excellent double-layer capacitance properties. However, due to the increasing demand for electrode materials, graphene has not been able to meet the performance requirements of people. Therefore, transition metal oxides with high specific capacitance have attracted much attention, but their poor electrical conductivity limits their application. Therefore, the production of composite materials has become an inevitable trend [6-11].

As a new clean energy storage device, supercapacitors had attracted much attention in the field of new energy, and electrode materials are one of the key factors affecting their electrochemical performance. The two-dimensional Ti_3C_2 in the MXene family has the advantages of special layered structure, large specific surface area, low operating voltage and good wettability with electrolyte. The layered structure of Ti_3C_2 is very suitable for ion embedding and de-embedding, but the lamination is easy to stack, which leads to a great reduction in the transfer efficiency of electrolyte, resulting in its low specific capacity and limiting its electrochemical utilization rate. In recent years, Ti_3C_2 , as an excellent graphene-like matrix material, has attracted great attention from researchers, but its low specific capacitance hinders its application. Therefore, the production of composite materials has become an inevitable trend.

In general, metal oxides are widely used in electrochemical capacitors because of their higher energy density than traditional carbon materials and better electrochemical stability than conductive polymers. Metal oxides such as RuO_2 , MnO_2 , Co_3O_4 and V_2O_5 have been used in supercapacitors and show excellent electrochemical performance. RuO_2 has been widely studied because of its good pseudocapacitance. However, high price and toxicity limit the application of RuO_2 . Therefore, researchers are actively seeking electrode materials with stable chemical properties, high specific capacity and low cost. A large number of studies have shown that the composite of TiO_2 and two-dimensional nanomaterials can significantly improve the electrochemical performance of electrode materials. TiO_2 is non-toxic, environmentally friendly, high chemical stability, low cost and has pseudocapacitance characteristics, all of which make it a research hotspot of electrode materials for supercapacitors [12]. Therefore, TiO_2 with stable chemical properties, high specific surface area, non-toxic, abundant natural reserves and low price was selected in this experiment.

In recent years, NiCo_2S_4 has been used as an electrode material for supercapacitors due to its high conductivity, rich redox reaction and larger specific capacitance than single metal sulfide [13-15].

However, when it is used independently as electrode material, it has some unignorable shortcomings such as poor electrochemical cycling stability. A large number of experiments show that the electrochemical properties of the electrode materials can be effectively improved by the combination of NiCo₂S₄ nanomaterials with a variety of materials [16-18]. Liu et al. successfully prepared NiCo₂S₄ nanotubes grown on carbon cloth with a simple two-step method. Ni(NO₃)₂·6H₂O, Co(NO₃)₂·6H₂O and urea were used as raw materials to obtain NiCo-precursor by hydrothermal method, and then Na₂S and the precursor were recombined by hydrothermal method to obtain NiCo₂S₄ nanotubes. The current density is 0.5 A/g and the specific capacitance can reach 578 F/g [19].

In this study, in order to obtain capacitors with high performance, Ti₃C₂ nanomaterial was modified in this experiment, and TiO₂-NiCo₂S₄-Ti₃C₂ composite material was prepared by simple and efficient hydrothermal reaction. A series of methods were used to characterize the composites, and electrochemical tests were carried out to analyze their electrochemical properties.

2. EXPERIMENTAL SECTION

2.1. Materials

NiCl₂·6H₂O and CoCl₂·6H₂O were purchased from Shanghai Qiangshun Chemical Reagent Co., Ltd and CH₅N₃S was purchased from Aladdin. Ti₃C₂ was purchased from Ningbo Jinlei Nanomaterials Technology Co., Ltd and was used as the substrate. Ethanol (C₂H₅OH) and Potassium hydroxide (KOH) were obtained from Sinopharm Chemical Reagent Co., Ltd. All the chemicals were analytical grade and used without further purification. Deionized water was used throughout the experiment.

2.2. Materials preparation

2.2.1. Synthesis of TiO₂-Ti₃C₂

0.75 g Ti₃C₂ was dissolved in 75 mL ethanol by stirring until the solution was evenly mixed. Then, the solution was transferred into a 100 mL stainless steel autoclave, maintained at 120 °C for 16 h. After cooling to room temperature in autoclave, the precipitate was repeatedly washed with ethanol solution and then dried in oven at 80 °C, the final product was TiO₂-Ti₃C₂.

2.2.2. Synthesis of NiCo₂S₄-Ti₃C₂

0.4754 g NiCl₂·6H₂O, 0.9516 g CoCl₂·6H₂O and 0.6174 g Ti₃C₂ were dissolved in 60 mL deionized water, and 0.7292 g CH₅N₃S was added to the above solution for ultrasonic degradation until uniformity. The solution was then transferred to a 100 mL stainless steel autoclave and kept under the condition of 180 °C for 12 h. After cooling to room temperature, it was removed and washed with deionized water and ethanol solution for several times, and then dried in an oven at 80 °C to obtain NiCo₂S₄-Ti₃C₂ composite material.

2.2.3. Synthesis of $\text{TiO}_2\text{-NiCo}_2\text{S}_4\text{-Ti}_3\text{C}_2$

0.5 g $\text{NiCo}_2\text{S}_4\text{-Ti}_3\text{C}_2$ was dissolved in 25 mL ethanol and stirred for 30 min. The obtained mixture solution was transferred to a 100 mL stainless steel autoclave for 16 h, and the temperature was kept at 120 °C. When the hydrothermal reaction was complete, the autoclave was cooled to ambient temperature. The precipitate was washed with ethanol solution and dried at 60 °C for 24 h under vacuum condition to obtain $\text{TiO}_2\text{-NiCo}_2\text{S}_4\text{-Ti}_3\text{C}_2$ composite.

2.3. Material characterization

The scanning electron microscope (SEM) images of samples were performed by a scanning electron microscopy. X-ray diffraction (XRD, PW3040/60, PANalytical B.V, and the scanning range of 2θ is 5 ° to 90 °) was used to determine the substance contained in the composite materials.

2.4. Electrodes preparation and electrochemical measurement

The whole electrochemical measurements including CV, GCD and EIS were measured by electrochemical workstation (CHI760E, China) using a conventional three-electrode system. The composite material was used as working electrode, a platinum gauze electrode and saturated calomel electrode were used as the counter electrode and the reference electrode respectively. The as-prepared materials were mixed with PVDF and acetylene black at a mass ratio of 8:1:1, and 2 mL isopropyl alcohol was added as a dispersant agent to form the mixed solution which was stirred thoroughly by ultrasonic shock. The obtained mixture was evenly coated with a pipette gun on the nickel foam with an area of 1 cm×1 cm and dried in a vacuum oven at 60 °C for 12 h. The exposed geometric area of the working electrode for electrochemical test was about 1×1 cm². All the electrochemical tests were conducted in 6 mol/L KOH aqueous electrolyte. In addition, special attention should be paid to the fact that the three electrodes are in a relatively high position and cannot contact each other during the experiment. The three electrodes can be completely immersed in the electrolyte and do not touch the cup wall. The samples were tested by cyclic voltammetry (CV), galvanostatic charge-discharge (GCD) and electrochemical impedance spectroscopy (EIS).

The cyclic voltammetry was tested by varying the scan rate from 5 to 80 mV/s. The measuring voltage range of charge and discharge was carried out in a range from 0 to 0.35 V which was as the same as that in CV. The current densities of 2.0 A/g, 3.0 A/g, 4.0 A/g, 6.0 A/g and 8.0 A/g were tested. According to the cyclic voltammetry, the specific capacitance of the electrode was calculated based on the following equation:

$$C_s = \frac{\int IdV}{2m \cdot v \cdot \Delta V} \quad (1)$$

where C_s (F/g) is the specific capacitance (F/g), I is the current (A), m is the quality of electrode material (g), v is the sweep speed (V/s) and ΔV is the range of voltage (V). The electrochemical impedance spectroscopy (EIS) measurements were measured in the range from 100 kHz to 0.01Hz.

3. RESULTS AND DISCUSSION

The morphologies of the samples were characterized by scanning electron microscopy (SEM), the SEM images of the obtained composites are shown in Fig. 1. As shown in Fig. 1A, it can be clearly seen that Ti_3C_2 presents a typical hand-wind instrument like multilayer, with clear and large interlayer spacing and smooth lamellar surface. As can be seen in Fig. 1B, with the addition of transition metal oxide particles, TiO_2 particles prepared by hydrothermal method were loaded on the accordion-like Ti_3C_2 nanoplates with the form of sphere. The layered structure of Ti_3C_2 is beneficial to the successful load of the transition metal oxide particles. From Fig. 1C, NiCo_2S_4 nanoparticles prepared by hydrothermal method are exposed around Ti_3C_2 in the form of flower buds. As can be seen from Fig. 1D, NiCo_2S_4 and TiO_2 nanoparticles are well combined with the matrix, which is conducive to the increase of the specific surface area of the material and the contact area between the active material and the electrolyte, so as to improve the electrochemical performance of the composite.

The diffractograms of the X-ray diffraction patterns of as-prepared samples were shown in Fig. 2. Fig. 2A shows XRD patterns of Ti_3C_2 , $\text{TiO}_2\text{-Ti}_3\text{C}_2$ and $\text{NiCo}_2\text{S}_4\text{-Ti}_3\text{C}_2$. In Fig. 2A, there are obvious diffraction peaks of Ti_3C_2 at 7.1° , 17.037° and 61.7° , corresponding to the crystal planes of (002), (004) and (110) respectively. The vital diffraction peaks of TiO_2 around $2\theta = 25.281^\circ$, 37.8° , 48.049° , 53.89° , 55.06° and 62.688° correspond to the crystal planes of (101), (004), (200), (105), (211) and (204) of the TiO_2 phase (JCPDS 21-1272). There are five peaks around $2\theta = 26.831^\circ$, 31.589° , 38.319° , 50.463° and 55.33° which can be well consistent with (220), (311), (400), (511) and (440) planes of NiCo_2S_4 (JCPDS 20-0782) respectively. In Fig. 2B, the XRD pattern of $\text{TiO}_2\text{-NiCo}_2\text{S}_4\text{-Ti}_3\text{C}_2$ nanomaterial is the superposition of Ti_3C_2 , $\text{TiO}_2\text{-Ti}_3\text{C}_2$ and $\text{NiCo}_2\text{S}_4\text{-Ti}_3\text{C}_2$, and no other impurity phase is detected. It indicates that the sample has high purity and $\text{TiO}_2\text{-NiCo}_2\text{S}_4\text{-Ti}_3\text{C}_2$ nanomaterial has been successfully prepared [20].

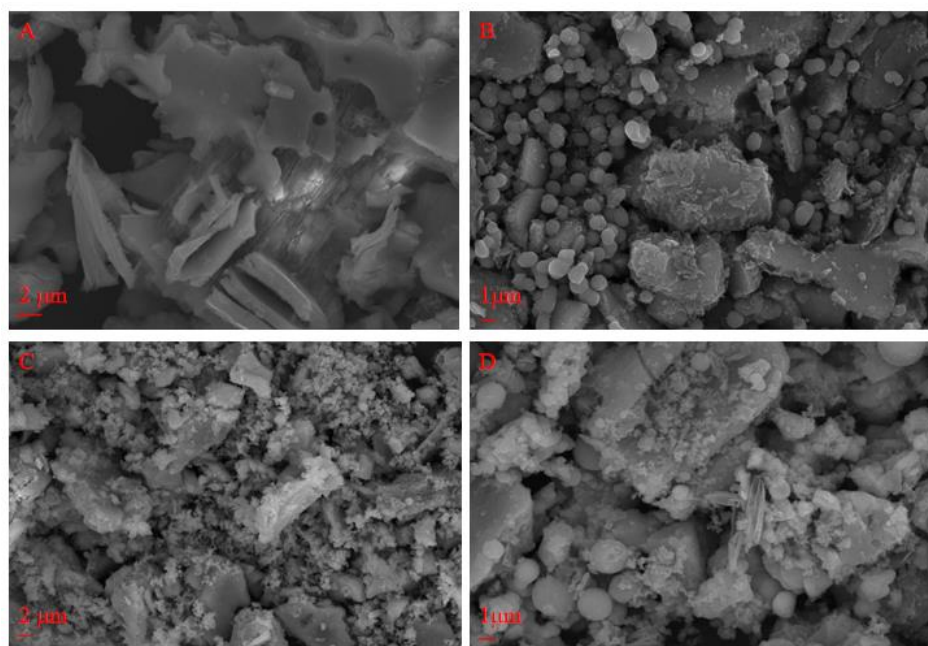


Figure 1. The SEM images of (A) Ti_3C_2 , (B) $\text{TiO}_2\text{-Ti}_3\text{C}_2$, (C) $\text{NiCo}_2\text{S}_4\text{-Ti}_3\text{C}_2$, (D) $\text{TiO}_2\text{-NiCo}_2\text{S}_4\text{-Ti}_3\text{C}_2$.

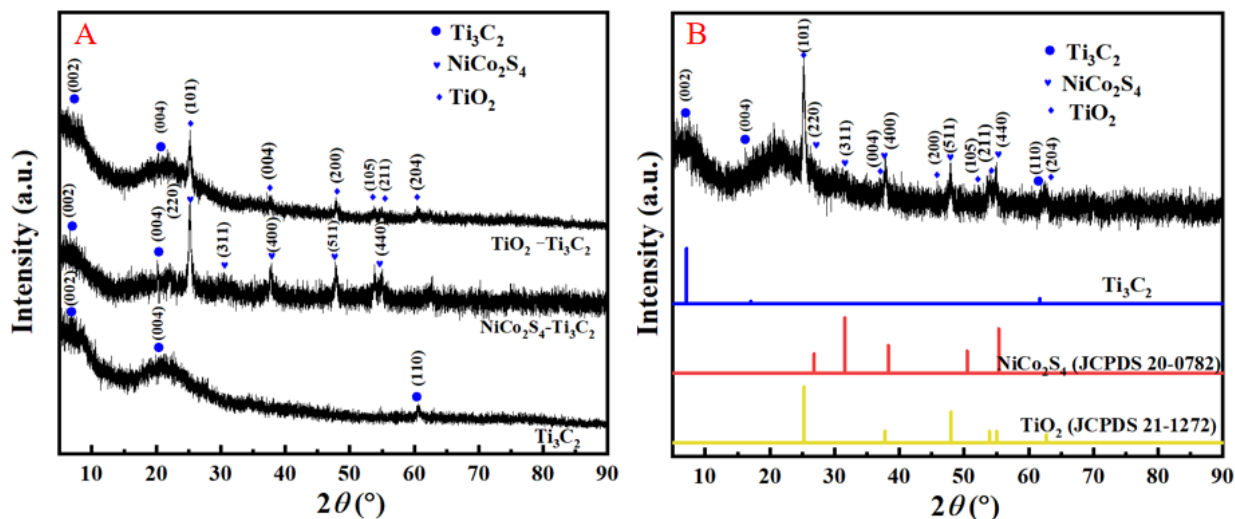


Figure 2. XRD patterns of (A) Ti_3C_2 , $\text{TiO}_2\text{-Ti}_3\text{C}_2$, $\text{NiCo}_2\text{S}_4\text{-Ti}_3\text{C}_2$, (B) $\text{TiO}_2\text{-NiCo}_2\text{S}_4\text{-Ti}_3\text{C}_2$.

Fig. 3 shows the CV curves of Ti_3C_2 , $\text{TiO}_2\text{-Ti}_3\text{C}_2$, $\text{NiCo}_2\text{S}_4\text{-Ti}_3\text{C}_2$ and $\text{TiO}_2\text{-NiCo}_2\text{S}_4\text{-Ti}_3\text{C}_2$ electrodes which were tested in 6 M KOH and the potential window is 0~0.35V. Fig. 3A shows the CV curves of several electrodes at the scan rate of 5 mV/s in 6 M KOH solution, respectively. As observed, under the condition of the same scanning rate, $\text{TiO}_2\text{-NiCo}_2\text{S}_4\text{-Ti}_3\text{C}_2$ has the largest area among the four electrodes. The specific capacitance of electrode materials can also be judged based on the CV curve area. This indicates that $\text{TiO}_2\text{-NiCo}_2\text{S}_4\text{-Ti}_3\text{C}_2$ has higher specific capacitance and better cycle stability. Fig. 3B shows the CV curves of $\text{TiO}_2\text{-NiCo}_2\text{S}_4\text{-Ti}_3\text{C}_2$ in 6 M KOH with different scan rates (5 mV/s, 10 mV/s, 20 mV/s, 40 mV/s, 60 mV/s and 80 mV/s) at room temperature. It can be seen from the figure that with the increase of scanning rate, the area enclosed by CV curve also increases.

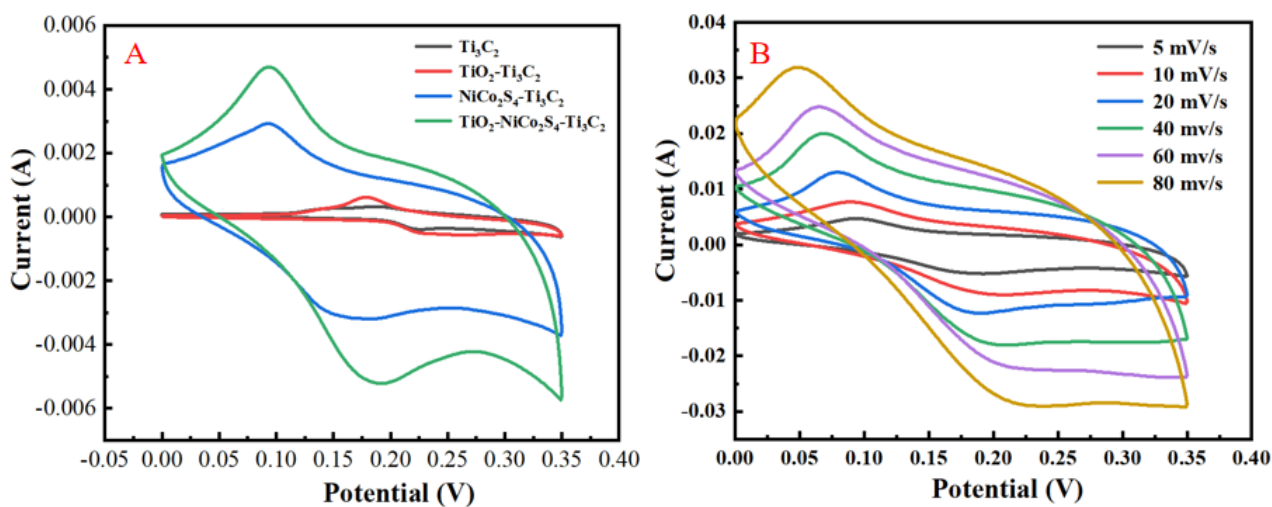


Figure 3. The cyclic voltammograms of (A) Ti_3C_2 , $\text{TiO}_2\text{-Ti}_3\text{C}_2$, $\text{NiCo}_2\text{S}_4\text{-Ti}_3\text{C}_2$, $\text{TiO}_2\text{-NiCo}_2\text{S}_4\text{-Ti}_3\text{C}_2$ in 6 M KOH at a scan of 5 mV/s, (B) $\text{TiO}_2\text{-NiCo}_2\text{S}_4\text{-Ti}_3\text{C}_2$ in 6 M KOH with different scan rates at room temperature.

Fig. 4 shows the constant current charge-discharge curves of these four electrodes at different current densities (2.0 A/g, 3.0 A/g, 4.0 A/g, 6.0 A/g, 8.0 A/g) in 6 M KOH. The GCD curves were shown in Fig. 4 (A-D) ranging from 0 to 0.35 V. It can be seen from the figures that the current density increases from right to left, the appearance of nonlinear shape with obvious discharge platforms represents typical pseudocapacitance characteristic and indicates that the electrode material has good reversibility of faraday redox [21]. Obviously, with the increase of current density, the charge and discharge time of each electrode decreases at the same time, leading to the active materials in the electrodes could not complete the Faraday electrochemical reaction at high current density [22]. Moreover, under the same current density, the charge and discharge time relationship of each composite electrode is $\text{TiO}_2\text{-NiCo}_2\text{S}_4\text{-Ti}_3\text{C}_2 > \text{NiCo}_2\text{S}_4\text{-Ti}_3\text{C}_2 > \text{TiO}_2\text{-Ti}_3\text{C}_2 > \text{Ti}_3\text{C}_2$. Under the same current density, $\text{TiO}_2\text{-NiCo}_2\text{S}_4\text{-Ti}_3\text{C}_2$ electrode has the longest charge and discharge time among these electrodes, indicating $\text{TiO}_2\text{-NiCo}_2\text{S}_4\text{-Ti}_3\text{C}_2$ has better capacitance performance. The electrochemical performance of ternary nanomaterials ($\text{TiO}_2\text{-NiCo}_2\text{S}_4\text{-Ti}_3\text{C}_2$) is better than that of binary and unit nanomaterials due to the successful combination of metal oxides and metal sulfides.

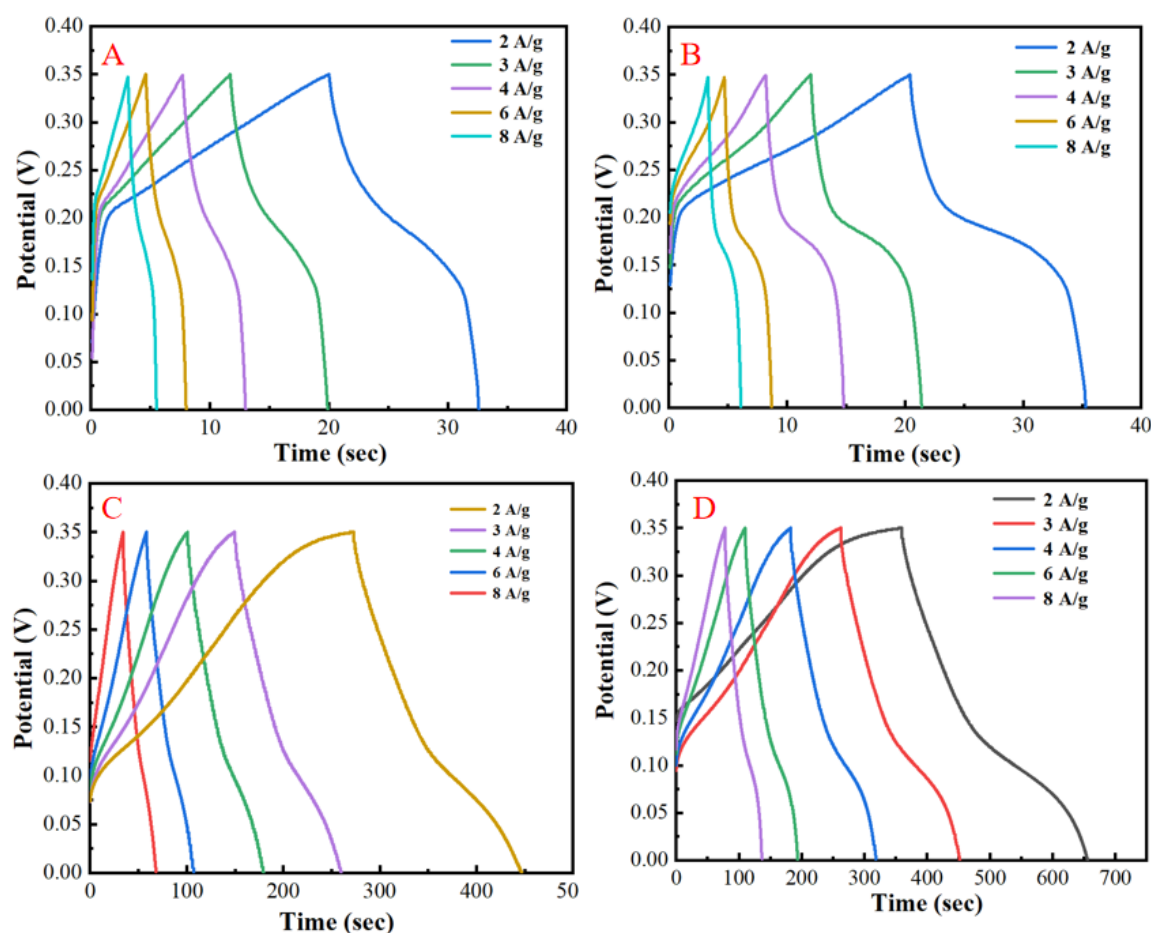


Figure 4. Charge and discharge curves of (A) Ti_3C_2 , (B) $\text{TiO}_2\text{-Ti}_3\text{C}_2$, (C) $\text{NiCo}_2\text{S}_4\text{-Ti}_3\text{C}_2$ and (D) $\text{TiO}_2\text{-NiCo}_2\text{S}_4\text{-Ti}_3\text{C}_2$ in 6 M KOH with different current densities

Fig. 5A shows the specific capacitance (C_{sp}) of Ti_3C_2 , $\text{TiO}_2\text{-Ti}_3\text{C}_2$, $\text{NiCo}_2\text{S}_4\text{-Ti}_3\text{C}_2$ and $\text{TiO}_2\text{-NiCo}_2\text{S}_4\text{-Ti}_3\text{C}_2$ electrodes at different scanning rates. The value of specific capacitance decreases with

the increase of scanning rate, which is directly related to the type of electrolyte ions and the diffusion process on the electrode surface [23]. Compared with the other three materials, the specific capacitance of $\text{TiO}_2\text{-NiCo}_2\text{S}_4\text{-Ti}_3\text{C}_2$ electrode material is largest. According to the trend of the curve, the maximum specific capacitance of $\text{TiO}_2\text{-NiCo}_2\text{S}_4\text{-Ti}_3\text{C}_2$ electrode material is 1527.5 F/g, and the specific capacitance relationship between each electrode can be written as $\text{TiO}_2\text{-NiCo}_2\text{S}_4\text{-Ti}_3\text{C}_2 > \text{NiCo}_2\text{S}_4\text{-Ti}_3\text{C}_2 > \text{TiO}_2\text{-Ti}_3\text{C}_2 > \text{Ti}_3\text{C}_2$, which is consistent with cyclic voltammetry and constant current charge and discharge results. Fig. 5B shows the EIS spectrum of Ti_3C_2 , $\text{TiO}_2\text{-Ti}_3\text{C}_2$, $\text{NiCo}_2\text{S}_4\text{-Ti}_3\text{C}_2$ and $\text{TiO}_2\text{-NiCo}_2\text{S}_4\text{-Ti}_3\text{C}_2$ electrodes in 6 M KOH. According to the comparison of the relation in the figure, among the four composite electrodes, the relation of the tilting degree of the four electrodes is $\text{TiO}_2\text{-NiCo}_2\text{S}_4\text{-Ti}_3\text{C}_2 > \text{NiCo}_2\text{S}_4\text{-Ti}_3\text{C}_2 > \text{TiO}_2\text{-Ti}_3\text{C}_2 > \text{Ti}_3\text{C}_2$. However, in each electrode, the active site is related to the ionic diffusion resistance in the electrolyte. The results show that the reaction rate of electrolyte ions in $\text{TiO}_2\text{-NiCo}_2\text{S}_4\text{-Ti}_3\text{C}_2$ electrode is faster and the resistance of ion movement is reduced. It can be concluded that there are more electrochemical activity in $\text{TiO}_2\text{-NiCo}_2\text{S}_4\text{-Ti}_3\text{C}_2$ electrode [24].

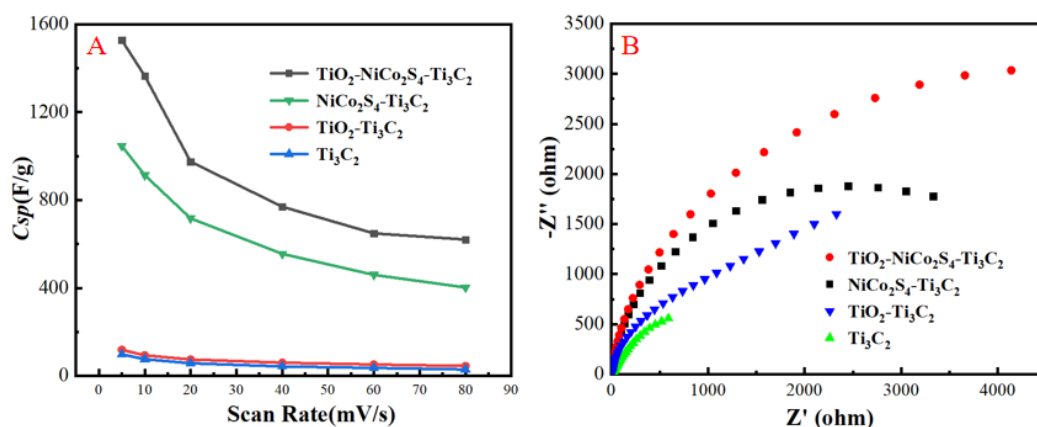


Figure 5. (A) The special capacitance diagram of Ti_3C_2 , $\text{TiO}_2\text{-Ti}_3\text{C}_2$, $\text{NiCo}_2\text{S}_4\text{-Ti}_3\text{C}_2$ and $\text{TiO}_2\text{-NiCo}_2\text{S}_4\text{-Ti}_3\text{C}_2$, (B) The electrochemical impedance spectroscopy of Ti_3C_2 , $\text{TiO}_2\text{-Ti}_3\text{C}_2$, $\text{NiCo}_2\text{S}_4\text{-Ti}_3\text{C}_2$ and $\text{TiO}_2\text{-NiCo}_2\text{S}_4\text{-Ti}_3\text{C}_2$ in 6 M KOH.

Table 1 compares the capacitance properties of synthesized materials in this paper with similar electrode materials.

Table 1. Comparison of the electrochemical performance of $\text{TiO}_2\text{-NiCo}_2\text{S}_4\text{-Ti}_3\text{C}_2$ in this work with previously reported studies.

Electrode Material	Test Solution	Specific capacitance/(F/g)	Reference
$\text{Ti}_3\text{C}_2/\text{MnO}_x$	1 M Li_2SO_4	602	[25]
$\text{Ti}_3\text{C}_2/\text{RGO}$	6 M KOH	1040	[26]
$\text{Ti}_3\text{C}_2/\text{PVA}$	1 M KOH	528	[27]
$\text{Ti}_3\text{C}_2/\text{PANI}$	3 M HCl	1353	[28]
$\text{Ti}_3\text{C}_2/\text{PPy}$	1 M H_2SO_4	1000	[29]
$\text{TiO}_2\text{-NiCo}_2\text{S}_4\text{-Ti}_3\text{C}_2$	6 M KOH	1527.5	This work

4. CONCLUSION

In this work, compared with Ti_3C_2 , $\text{TiO}_2\text{-Ti}_3\text{C}_2$ and $\text{NiCo}_2\text{S}_4\text{-Ti}_3\text{C}_2$, the prepared $\text{TiO}_2\text{-NiCo}_2\text{S}_4\text{-Ti}_3\text{C}_2$ composite has the largest specific capacitance as electrode material. At the scanning rate of 5 mV/s, the specific capacitance of $\text{TiO}_2\text{-NiCo}_2\text{S}_4\text{-Ti}_3\text{C}_2$ composite material can reach 1527.5 F/g, and the charge and discharge time of $\text{TiO}_2\text{-NiCo}_2\text{S}_4\text{-Ti}_3\text{C}_2$ composite material is the longest at the current density of 2 A/g. This fully shows that it has good conductivity. In conclusion, the composite of transition metal oxide TiO_2 and metal sulfide NiCo_2S_4 with Ti_3C_2 is beneficial to improve the electrical capacity of the material. Therefore, $\text{TiO}_2\text{-NiCo}_2\text{S}_4\text{-Ti}_3\text{C}_2$ is a composite material with good electrochemical performance for making chemical capacitors.

DECLARATION OF COMPETING INTEREST

The authors declare that we have no conflicts of interest.

ACKNOWLEDGEMENTS

This work was financially supported by Postgraduate Research & Practice Innovation Program of Jiangsu University of Technology (XSJCX21_74), Postgraduate Research & Practice Innovation Program of Jiangsu Province (Zhe Li, Haoyu Wang), Innovation and Entrepreneurship Training program for College students in Jiangsu Province (Haitao Liu), National Natural Science Foundation of China (grant no. 31800495), Natural Science Foundation of Jiangsu Province (grant no. BK20181040).

References

1. L. Liu, H. Zhang, L. Fang, Y. Mu and Y. Wang, *J. Power Sources*, 327 (2016) 135.
2. G. Zhang and X. Lou, *Surf. Sci. Rep.*, 3 (2013) 1470.
3. Z. Yu, L. Tetard, L. Zhai and J. Thomas, *Energy Environ. Sci.*, 8 (2015) 702.
4. Z. Li, A. Gu, Z. Lou, J. Sun, Q. Zhou and K. Chan, *J. Mater. Sci.*, 52 (2017) 4852.
5. F. Jiang, W. Li and R. Zou, *Nano Energy*, 7 (2014) 72.
6. Y. Zhang, Q. Zou and H. S. Hsu, *ACS Appl. Mater. Interfaces*, 11 (2016) 7363.
7. J. Tang, J. Shen and N. Li, *J. Alloys Compd.*, 666 (2016) 15.
8. J. Li, X. Zhang and J. Guo, *J. Alloys Compd.*, 674 (2016) 44.
9. M. S. Beatriz, T. Brousse and R. C. Claudi, *Electrochim. Acta*, 91 (2013) 253.
10. S. Bai, C. Chen and R. Luo, *Sens. Actuators, B*, 216 (2015) 113.
11. S. Bhattacharya, D. Dinda and S. K. Saha, *J. Phys. D: Appl. Phys.*, 48 (2015) 303.
12. S. C. Pang, M. A. Anderson and T. W. Chapman, *J. Electrochem. Soc.*, 147 (2000) 444.
13. L. Hou, H. Hua, R. Bao, Z. Chen, C. Yang, S. Zhu, G. Pang, L. Tong, C. Yuan and X. Zhang, *ChemPlusChem*, 81 (2016) 557.
14. Y. Zhu, X. Ji, Z. Wu and Y. Liu, *Electrochim. Acta*, 186 (2015) 562.
15. Y. Zhang, M. Ma, J. Yang, C. Sun, H. Su, W. Huang and X. Dong, *Nanoscale Adv.*, 6 (2014) 9824.
16. F. Yu, Z. Chang and L. J. Fu, *J. Mater. Chem. A*, 14 (2018) 5856.
17. X. R. Han and Q. Chen, L. Zhang, *Chem. Eng. J.*, 368 (2019) 513.
18. W. Wu, D. Niu and J. Zhu, *Ceram. Int.*, 45 (2019) 16261.
19. C. Liu and X. Wu, *Mater. Res. Bull.*, 103 (2018) 55.
20. X. Lu, X. Huang, S. Xie, T. Zhai, C. Wang, P. Zhang, M. Yu, W. Li, C. Liang and Y. Tong, *J. Mater. Chem.*, 22 (2012) 13357.

21. J. Z. Wu, X. Y. Li, Y. R. Zhu, T. F. Yi, J. H. Zhang and Y. Xie, *Ceram. Int.*, 42 (2016) 9250.
22. Y. R. Zhu, P. P. Peng, J. Z. Wu, T. F. Yi, Y. Xie and S. Luo, *Solid State Ionics*, 336 (2019) 110.
23. R. A. Davoglio, G. Cabello and J. F. Marco, *Electrochim. Acta*, 261 (2018) 428.
24. S. Y. Kim, J. H. Wee and C. M. Yang, *J. Electroanal. Chem.*, 801 (2017) 403.
25. Y. P. Tian, C. H. Yang, W. X. Que, X. B. Liu, X. T. Yin and L. B. Kong, *J. Power Sources*, 359 (2017) 332.
26. J. Yan, C. E. Ren, K. Maleski, C. B. Htter, B. Anasori, P. Urbankowski, A. Sarycheva and Y. Gogotsi, *Adv. Funct. Mater.*, 27 (2017) 1701264.
27. Z. Ling, C. E. Ren, M. Q. Zhao, J. Yang, J. M. Giammarco, J. S. Qiu, M. W. Barsoum and Y. Gogotsi, *PNAS*, 111 (2014) 16676.
28. A. V. Mohammadi, J. Moncada, H. G. Chen, E. Kayali, J. Orangi, C. A. Carrero and M. Beidaghi, *J. Mater. Chem. A*, 6 (2018) 22123.
29. M. Boota, B. Anasori, C. Voigt, M. Q. Zhao, M. W. Barsoum and Y. Gogotsi, *Adv. Mater.*, 28 (2015) 1517.

© 2022 The Authors. Published by ESG (www.electrochemsci.org). This article is an open access article distributed under the terms and conditions of the Creative Commons Attribution license (<http://creativecommons.org/licenses/by/4.0/>).